

# Synthesis, characterization, and thermal study of polyaniline composite with the photoadduct of potassium hexacyanoferrate (II) involving hexamine ligand

Mohammad Sideeq Rather · Kowsar Majid ·  
Ravinder Kumar Wanchoo · Madan Lal Singla

Received: 1 November 2011 / Accepted: 13 July 2012 / Published online: 26 August 2012  
© Akadémiai Kiadó, Budapest, Hungary 2012

**Abstract** The present paper involves the synthesis of polyaniline (PANI) composite with photoadduct of potassium hexacyanoferrate (II) involving hexamine as a ligand and cobalt chloride as a complexing agent via in situ oxidative polymerization by ammonium persulphate. The photoadduct has been synthesized by photoirradiation followed by substitution with the hexamine ligand. The final product has been isolated by using  $\text{CoCl}_2$  as complexing agent. Viscosity average molar mass has been determined by viscosity method using Ostwald's viscometer. The photoirradiation, substitution, and successful synthesis have been proved by recording pH, UV–visible spectra before and after irradiation, and FTIR of the photoadduct. The composite based on the synthesized photoadduct has been subjected to FTIR, X-ray diffraction, and SEM characterization techniques. Thermal analysis has been done by using TG and DSC technique. FTIR absorption peaks confirm the insertion of photoadduct in the backbone of PANI. SEM of the composite also supports its successful synthesis. The XRD of photoadduct shows crystalline structure, which has remained dominant in the composite, hence proving the successful

synthesis of PANI composite with photoadduct. Thermal analysis shows high thermal stability of photoadduct which in turn has improved the thermal stability of PANI composite, therefore, shows the potential of composite for high-temperature application purposes.

**Keywords** Polyaniline · Hexacyanoferrate (II) · Hexamine · Photoadduct · Photoirradiation

## Introduction

Conjugated polymers containing transition metal complexes are the most attractive systems under observation of material scientist [1]. These types of systems are also called as hybrid polymers as they contain both organic and inorganic moieties. These systems are attractive because the resulting material possesses many physical properties [2–4]. These properties arise because of the ability of transition metals to bind with anions, small molecules or ligands [5–7]. Transport of electrons, from metal to ligand also gives rise to various interesting features of these complexes. As a consequence, these materials find applications in various fields like catalysis, sensors, and medical applications [8–10].

Certain systems possess chain–chain interactions, which can give rise to bulk conductivity and are reported to display high conductivity [11, 12]. Interaction in conjugated polymer chains is also because of  $\pi$  aggregations. In these aggregates, the polymers are in direct electronic communication with one another through weak, cofacial  $\pi$ -bonds between the aromatic rings [13, 14]. In some cases, it has been reported that there exists a strong interaction between transition metal complex, ligand, and conducting polymer backbones which result in unique properties and applications

---

M. S. Rather · K. Majid (✉)  
Department of Chemistry, National Institute of Technology,  
Srinagar 190 006, Jammu and Kashmir, India  
e-mail: kowsarmajid@yahoo.co.in; kowsarmajid@rediffmail.com

R. K. Wanchoo  
Department of Chemical Engineering Punjab University,  
Chandigarh 160 014, India

M. L. Singla  
Material Research Division, Central Scientific Instruments  
Organization (CSIO), CSIR Sector-30C, Chandigarh 160 030,  
India

**Table 1** Parameters for calculating average molecular weight

Concentration/g cm <sup>-3</sup>	Time/s	$\eta_{red}$	$\eta_{sp}$	$\eta_{red}$
0.003	100	1.204	0.204	68
0.006	120	1.445	0.44	73.3
0.009	140	1.686	0.686	76.22

[15, 16]. In this direction, a series of novel conjugated polymers containing mixed-ligand ruthenium complexes have been synthesized, characterized, and investigated for their photoconductive properties [17]. Polythiophene hybrids of transition metal bis(salicylaldehyde) has been reported, where  $\pi$  aggregation processes are shown to occur [18]. Great efforts have been focused on development of low cost solar cell based on hybrid conjugated polymers [19].

Among conducting polymers, polyaniline (PANI) has been widely studied because of its stability, good conductivity at room temperature, and other potential applications [20–22]. Various composites of PANI with various fillers, binders, and dopants have been synthesized, characterized, and explored for various applications. However, very few reports are available regarding preparation and characterization of transition metal-based PANI hybrid systems. This has remained as one motivation behind investigation of this work (Table 1).

The other aspect of this study is very fascinating, labile, and easy route of synthesis of photoadducts through photochemical procedure. Photochemistry of transition metal complexes especially cyanocomplexes possess a beautiful and flexible route for further substitution and addition reactions. The kinetics and mechanistic studies of these photo-substituted reactions have been discussed extensively in literature [23–26]. Photoreactivity of octacyanometallates of Mo(IV), W(IV), and Fe(III) with many ligands like 2,2'-bipyridyl, 1,10'-phenanthroline, ethylenediamine, 8-hydroxyquinoline, pyrazine, ethanolamine, imidazole has been reported [27–30]. The intermediate photoaquation reactions of these cyanocomplexes undergo substitution reactions with various ligands and provide an easy route of incorporation of desired ligands into the complex. The final product has been isolated as such, or as an adduct, by the addition of some other complexing agent or metal chloride solution. The final product, more appropriately a photoadduct, represents a combination of metal center with very potent ligands. The photoadduct as a whole possess very significant properties which can be incorporated into the polymer matrix in order to improve upon the various characteristic features of the polymer matrix. In this direction, potassium hexacyanoferrate (II) has been chosen for investigation because of the fact that photoirradiation in the ligand field bands of hexacyanoferrate (II) in an alkaline medium results in the substitution

of cyanide ligand by water followed by other thermal steps, which results in the formation of stable products with ligands 2,2'-bipyridyl, 1,10'-phenanthroline, imidazole, etc. These materials act like hybrid materials and have found innumerable applications in technological, medical, and industrial fields. Moreover,  $K_4Fe(CN)_6$  is easily available among all cyanocomplexes and is photochemically active. Keeping in view the potential application of these compounds, the synthesis of photoadduct from  $K_4Fe(CN)_6$  with hexamethylenetetramine commonly known as hexamine has been taken into account. The choice of hexamine is because of its good solubility, coordinating property, and wide range of industrial applications. Therefore, we are here reporting the synthesis of hybrid polymer composites of PANI with photoadduct of potassium hexacyanoferrate (II), and hexamine. The material synthesized has been subjected to various spectroscopic characterization techniques. Surface characterization has been done by SEM. Thermal study of the material has also been carried out.

## Experimental

### Materials

Aniline was supplied by Loba Chemicals and was used after distillation HCl, ammonium persulphate was also provided by Loba chemicals. All other reagents used were of analytical reagent grade. All solutions were prepared in triply distilled water.

### Physical measurements

UV–visible spectra were taken on Shimadzu UV-190 double-beam spectrophotometer. Irradiation was done with the help of Osram UV photolamp. Fourier transform infrared (FTIR) spectra were recorded on Perkin Elmer RX-1 FTIR spectrophotometer. The spectra were taken in KBr disks. Surface morphology of the samples was studied on a Hitachi SEM Model S-3600N. X-ray diffraction (XRD) was recorded on PW 3050 base diffractometer with Cu-K $\alpha$  radiations (1.54060 Å). Thermogravimetric analysis coupled with DSC was carried out with universal TA instruments V4.5A in an argon atmosphere at a heating rate of 10 °C min<sup>-1</sup>. The temperature range was from ambient to 1,200 °C. An aluminum pan was used as a reference. The DSC was calibrated by the fusion of indium (99.99 % purity); temperature repeatability of TA is  $\pm 0.1$  °C and  $\Delta H$  is  $\pm 0.02$  mW. The experimental procedure involves placing of 15.33 mg of sample in a pan, setting the pressure and heating rate. In this procedure, material was subjected to a linear temperature programme and the rate of heat flow into the material was continuously measured with increase

in temperature. The temperature difference as a function of time shows peaks as heat is either absorbed or released by the sample under examination.

### Synthesis of photoadducts

Aqueous solutions of  $\text{K}_4\text{Fe}(\text{CN})_6$  and hexamine were mixed in equimolar ratio (0.3 mol). The solution mixtures were subjected to UV radiation using Osram UV photolamp for about half an hour till the color of solution changed to deep yellow. Aqueous solution of cobalt chloride was added dropwise until a greenish precipitate was formed. The precipitate resulting from this solution was filtered and washed repeatedly in Buckner funnel under vacuum with distilled water. The precipitate now called photoadduct was collected and dried in an oven at about 40 °C. The photoadduct was finally isolated and dried over fused  $\text{CaCl}_2$ .

### Synthesis of PANI

PANI was prepared by known methods of oxidation with ammonium persulphate  $(\text{NH}_4)_2\text{S}_2\text{O}_8$ . To precooled solution of 10 ml distilled aniline dissolved in 150 ml of distilled water with 10 ml concentrated HCl, 4.5 g of  $(\text{NH}_4)_2\text{S}_2\text{O}_8$  dissolved in 30 ml of water was added dropwise to the solution with constant stirring. The solutions were kept stirring for about 2 h and were left for more than 1 h. The precipitate resulting from this solution was filtered and washed repeatedly in Buckner funnel under vacuum with distilled water. The precipitate was collected and dried in an oven at about 40 °C.

### Synthesis of photoadduct-based composites of PANI

To precooled solutions of 10 ml distilled aniline dissolved in 150 ml of distilled water with 10 ml concentrated HCl, 2.5 g of photoadduct was added into the solution with constant stirring. To this solution, 4.5 g of  $(\text{NH}_4)_2\text{S}_2\text{O}_8$  dissolved in 30 ml of water was added dropwise with constant stirring. The solution was kept stirring for about 2 h and was left for more than 1 h. The precipitate resulting from this solution was filtered and washed repeatedly in Buckner funnel under vacuum with distilled water. The precipitate was collected and dried in an oven at about 40 °C.

## Results and discussions

### Determination of viscosity average molecular weight

In order to determine the viscosity average molecular weight of composite, we prepared solution of 0.003, 0.006,

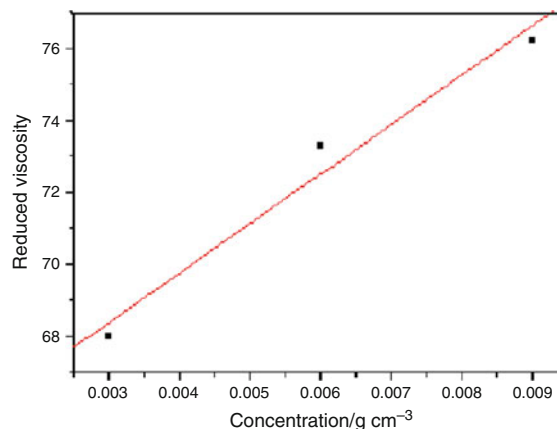


**Fig. 1** Plot of reduced viscosity versus  $c$

0.009, concentration ( $c$ ,  $\text{g cm}^{-3}$ ) in 10 ml of 1-methyl-2-pyrrolidone (NMP). The reduced viscosities of these samples were determined at 25 °C in NMP, using an Ostwald's viscometer; average molecular weight of composite was calculated using the Mark–Kuhn–Houwink–Sakurada equation:

$$[\eta] = K(M)^\alpha \quad (1)$$

where  $M$  is the viscosity average molar mass,  $K$  and  $\alpha$  are constants. In the present case  $K = 1.95 \times 10^{-6}$ , and  $\alpha = 1.36$ ,  $[\eta]$  is intrinsic viscosity also called viscosity number or Staudinger index and is related to other quantities as  $[\eta] = \lim_{C \rightarrow 0} n_{sp}/C$  when  $C \rightarrow 0$ ,  $n_{red} = n_{sp}/C$ ,  $n_{sp} = n_{rel} - 1$ , and  $n_{rel} = t/t_0$ , where  $n_{red}$  is the reduced viscosity,  $n_{sp}$  is the specific viscosity, and  $n_{rel}$  is the relative viscosity,  $t$  and  $t_0$  are viscometer drain times of solution and solvent, respectively.  $\eta_{red}$  was then plotted versus the composite concentration for three concentrations, and a linear extrapolation to zero concentration produced the value of  $[\eta] = 67.7$  (Fig. 1). After putting the values of  $[\eta]$ ,  $K$ , and  $\alpha$  in the Mark–Houwink equation (1), the viscosity average molecular weight of the PANI composite comes out to be 354,813.

### UV characterization

When aqueous  $[\text{Fe}(\text{CN})_6]^{4-}$  solution is irradiated with UV or visible light,  $\text{Fe}^{+2}$  ions and HCN were product with the increase in pH of the solution. The pH of equimolar solution of  $[\text{Fe}(\text{CN})_6]^{4-}$  and hexamine before and after irradiation was 9.77 and 11.22, respectively, which shows successful photoaquation. The photoirradiation followed by substitution was further proved by recording UV–Vis spectra of this solution before and after irradiation (Fig. 2). Before irradiation, the peaks observed are at 397 nm can be assigned as spin allowed ligand field transition  ${}^1\text{A}_{1g} \rightarrow {}^1\text{T}_{1g}$  which shows a shift after irradiation by

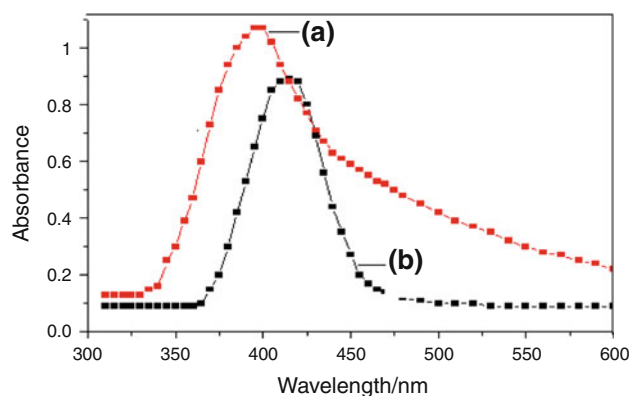


**Fig. 2** UV-Vis spectra of potassium hexacyanoferrate with hexamine (0.01 M each) (A) before irradiation and (B) after irradiation

appearing at 415 nm which can be assigned to the  $^1A_{1g} \rightarrow ^3T_{1g}$  spin forbidden ligand field transition.

### FTIR characterization

In order to understand the FTIR of photoadduct, we recorded the FTIR spectra of  $K_4Fe(CN)_6$  and hexamine individually, and compared it with FTIR spectra of photoadduct (Fig. 3a–c). The successful photoirradiation with consequent substitution by hexamine is clear from the spectra. Cyanocomplexes exhibit sharp  $\nu$  ( $-C\equiv N$ ) stretching bands at  $2,170$ – $2,030\text{ cm}^{-1}$ . The characteristics peaks of  $\nu$  ( $-C\equiv N$ ) in case of  $K_4Fe(CN)_6$  appears at  $2,030\text{ cm}^{-1}$ .

The absorption peaks because of H–O–H outside the sphere, i.e., lattice water, will be bound to the crystal by weak forces and it has been found to show absorption peaks at  $3,550$ – $3,200\text{ cm}^{-1}$  (due to antisymmetric and symmetric stretching modes) and at  $1,630$ – $1,600\text{ cm}^{-1}$  due to H–O–H bending mode. In case of photoadduct spectrum, we found an absorption band at  $3,399$  and  $1,627\text{ cm}^{-1}$ , which can be assigned to  $\nu$  (H–O–H) stretching and  $\nu$  (H–O–H) bending, respectively, hence, shows the presence of lattice water in the final photoadduct. The presence of this lattice water has been further confirmed from thermograms of photoadduct. It shows the mass loss of 6 % within the temperature range of  $80$ – $200\text{ }^\circ\text{C}$  as a result of expulsion of lattice water moiety.

The FTIR of pure hexamine is showing absorption peaks at  $1,460$  and  $1,364\text{ cm}^{-1}$  due to  $\nu$ - $CH_2$  bending, shows a shift to higher frequency and appears at  $1,464$  and  $1,381\text{ cm}^{-1}$ , hence, justifying the coordination of hexamine. The sharp peaks at  $1,236$  and  $1,046\text{ cm}^{-1}$  in photoadduct is due to symmetric and asymmetric  $\nu$  (C–N) of pure hexamine, have shifted to  $1,244$  and  $1,004\text{ cm}^{-1}$  with splitting in both peaks in photoadduct, also shows the presence of hexamine, with a different environment. Thus, the FTIR of photoadduct is showing the presence of

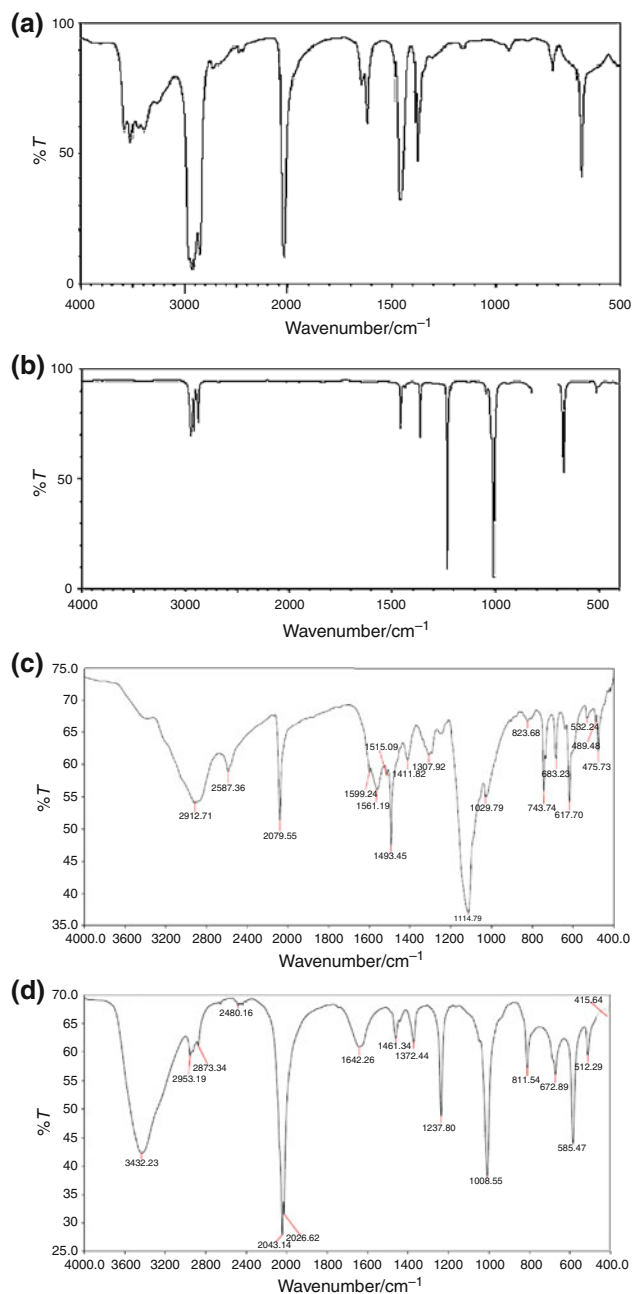


**Fig. 3** FTIR of **a** potassium hexacyanoferrate (II), **b** hexamine, **c** photoadduct of potassium hexacyanoferrate (II) with hexamine and  $CoCl_2$ , and **d** composite of potassium hexacyanoferrate with hexamine and  $CoCl_2$  in PANI

cyanide and hexamine moieties. The complexing with  $CoCl_2$  is reflected from the absorption peaks in the lower frequency region at  $593$ ,  $688$ , and  $807\text{ cm}^{-1}$ , because of the stretching vibrations of M–Cl.

For successful synthesis of PANI composite with synthesized photoadduct, we compare the FTIR of photoadduct and composite (Fig. 3c, d). PANI shows characteristic hump at  $3,305\text{ cm}^{-1}$  because of N–H stretching [31]. This hump appears at  $3,400\text{ cm}^{-1}$  but with a shift of  $95\text{ cm}^{-1}$  in

the composite. The absorption peaks of photoadduct due to  $\nu$  (H–O–H) stretching appear at  $3,399\text{ cm}^{-1}$  and overlaps with the hump due to PANI at  $3,400\text{ cm}^{-1}$ . This is more prominent in the composite and is hence showing the presence of photoadduct in the PANI chain. This hump extends and gives a broad absorption peak at  $2,912\text{ cm}^{-1}$ , which can be because of  $\nu$  (C–H) stretching due to PANI chain. This peak appears at  $2,922\text{ cm}^{-1}$  in the pure PANI. The insertion of photoadduct in the PANI is further evident by the appearance of sharp peak at  $2,079\text{ cm}^{-1}$ , which is due to  $\nu$  (C $\equiv$ N). This peak appears at  $2,080\text{ cm}^{-1}$  in the photoadduct but with a high intensity, therefore, justifying the coordination of photoadduct with the PANI. Moreover, the presence of photoadduct in the PANI chain is further confirmed by the appearance of all absorption peaks due to hexamine with some shifts. The absorption peak due to CH<sub>2</sub> bending appears at  $1,364$  and  $1,460\text{ cm}^{-1}$  in pure hexamine appears at  $1,307$ ,  $1,411$ , and  $1,493\text{ cm}^{-1}$  in the composite, showing significant shifts, justifying the coordination. The presence of metal chloride peaks at  $593$ ,  $688$ , and  $807\text{ cm}^{-1}$  in photoadduct appears at  $475$ ,  $617$ , and  $743\text{ cm}^{-1}$  in the composite.

Therefore, from the discussion of FTIR of pure hexamine, K<sub>4</sub>Fe(CN)<sub>6</sub>, photoadduct, pure PANI, and the composite of PANI with synthesized photoadducts, the successful synthesis of photoadduct and composite of PANI with this photoadduct is proved.

#### SEM characterization

The SEM image of pure PANI and composite is shown in Fig. 4a, b. SEM of pure PANI shows uniform chain structure while that of the composite shows the uniform distribution of crystalline photoadducts throughout the polymer chain. The PANI chain seems to engulf the photoadduct particles, therefore, images also support the successful synthesis of composite of PANI with this photoadduct.

#### XRD characterization

XRD of photoadduct and composite of PANI with photoadduct are shown in Fig. 5a, b. The XRD of PANI is showing the amorphous structure by the appearance of weak peak at  $2\theta$  value of  $20^\circ$  [31]. The XRD of photoadduct is having crystalline structure showing peaks at  $2\theta$  value of  $17.30^\circ$ ,  $24.75^\circ$ , and  $35.42^\circ$  with a relative intensity of  $80.37$ ,  $100$ , and  $59.44$ , respectively (Table 2). The XRD of composite of PANI with photoadduct is showing crystalline structure by the appearance of peaks at  $2\theta$  value of  $6.12^\circ$ ,  $12.14^\circ$ ,  $17.51^\circ$ ,  $18.26^\circ$ ,  $20.13^\circ$ ,  $21.15^\circ$ ,  $23.97^\circ$ ,  $24.81^\circ$ ,  $25.67^\circ$ ,  $27.48^\circ$ ,  $29.16^\circ$ ,  $31.04^\circ$ ,  $35.44^\circ$ ,  $37.00^\circ$ ,  $39.52^\circ$ , and  $57.40^\circ$  with a relative intensity of  $100$ ,  $1.95$ ,  $4.01$ ,  $22.21$ ,  $7.5$ ,  $3.46$ ,  $5.21$ ,  $3.39$ ,  $2.09$ ,  $0.66$ ,  $1.42$ ,  $1.77$ ,

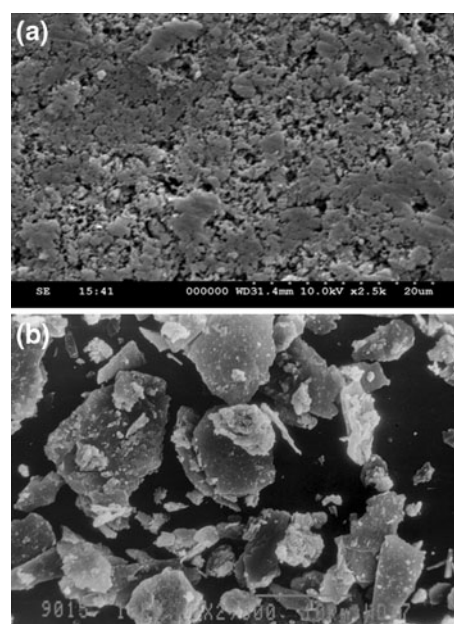


**Fig. 4** SEM image of **a** pure PANI, **b** composite of potassium hexacyanoferrate with hexamine and CoCl<sub>2</sub> in PANI

$1.39$ ,  $1.24$ ,  $0.72$ , and  $0.43$ , respectively (Table 3). It is evident that the amorphous structure has changed into crystalline one with a number of significant peaks. Among these, peaks appearing at  $2\theta$  values of  $17.3098^\circ$ ,  $24.7505^\circ$ , and  $35.423^\circ$  due to photoadduct have appeared in the composite at  $2\theta$  value of  $17.5124^\circ$ ,  $24.8168^\circ$ , and  $35.442^\circ$ , respectively, showing the successful insertion of photoadduct into the composite. Moreover, the pure PANI being amorphous shows a hump at  $2\theta$  value of  $20^\circ$  is also appearing at  $20.1389^\circ$  in case of composite. In addition to this, many peaks are observed in the composite which demonstrates the change of structure from amorphous to crystalline one.

#### Thermal analysis

The TG/DSC of PANI, photoadduct of K<sub>4</sub>Fe(CN)<sub>6</sub> with hexamine, and composite of PANI with synthesized photoadduct, are shown in Fig. 6a, b, and c, respectively. The TG of PANI shows two transitions, the first one because of expulsion of certain amount of water. The temperature range of this transition is  $18$ – $85^\circ\text{C}$  with a mass loss of  $4.33\%$ , which indicates that the moisture must be embedded in the outer layers of material. The second transition initiates from  $278^\circ\text{C}$  and ends at  $590^\circ\text{C}$ , with a mass loss of  $49.82\%$ , which is because of release of organic moieties like C, H, and N. The decomposition is  $87.43\%$  in case of air atmosphere showing complete decomposition of PANI [31]. DSC of PANI shows two transitions corresponding to two transitions of TG curve.

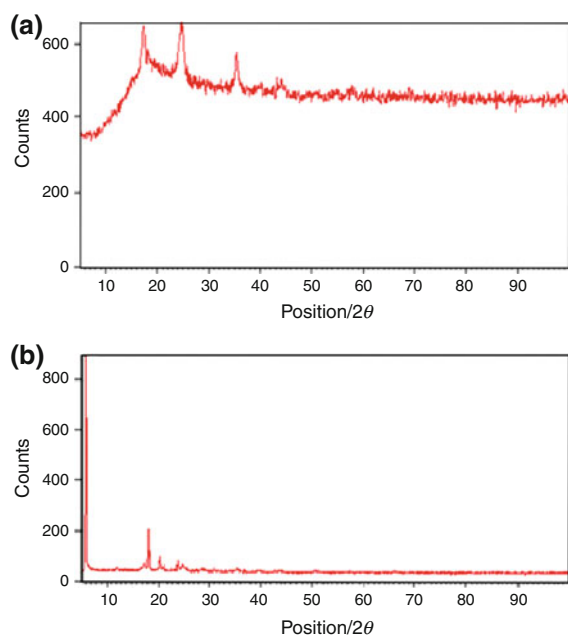


**Fig. 5** XRD of **a** photoadduct of potassium hexacyanoferrate with hexamine and  $\text{CoCl}_2$ , **b** composite of potassium hexacyanoferrate with hexamine and  $\text{CoCl}_2$  in PANI

**Table 2** XRD data of photoadduct of potassium hexacyanoferrate with hexamine and  $\text{CoCl}_2$

Pos./ $^{\circ}2\theta$	FWHM/ $^{\circ}2\theta$	$d$ -spacing/ $\text{\AA}$	Rel. int/ %	Area/cts* $^{\circ}2\theta$ .
17.3098	0.4684	5.12311	80.37	53.76
24.7505	0.6691	3.59724	100.00	95.57
35.4231	0.4015	2.53410	59.44	34.09

Both these transitions are endothermic. TG curve of photoadduct is showing three transitions. The first transition starts from ambient temperature and stops at  $100\text{ }^{\circ}\text{C}$ , with a mass loss of 6 % which is as a result of the loss of lattice water molecules. The same has been confirmed from FTIR of photoadduct, in which an absorption band at  $3,399\text{ cm}^{-1}$  and a peak at  $1,627\text{ cm}^{-1}$  has appeared which are due to stretching and bending modes of lattice water. The second transition initiates from  $278\text{ }^{\circ}\text{C}$  and ends at  $425\text{ }^{\circ}\text{C}$ , with a mass loss of 24 %, which is because of release of organic moieties like C, H, and N from hexamine and cyanide ligands. The curve shows stability up to  $550\text{ }^{\circ}\text{C}$  where from third transition initiates and ends at  $920\text{ }^{\circ}\text{C}$  with a mass loss of about 18 % which may be because of removal of some inorganic moieties. The residue left behind at this temperature is 20 % which shows stability up to  $1,200\text{ }^{\circ}\text{C}$ , showing the significant thermal stability of synthesized photoadduct.

The DSC of photoadduct is showing two transitions, first one an exothermic transition, starts from ambient temperatures to  $500\text{ }^{\circ}\text{C}$  with a maximum at  $374.94\text{ }^{\circ}\text{C}$  and enthalpy

**Table 3** XRD data of composite of potassium hexacyanoferrate with hexamine and  $\text{CoCl}_2$  in PANI

Pos./ $^{\circ}2\theta$ .	FWHM/ $^{\circ}2\theta$	$d$ -spacing/ $\text{\AA}$	Rel. int./ %	Area/cts* $^{\circ}2\theta$ .
6.1291	0.1840	14.4204	100	1341.04
12.1433	0.1338	7.28864	1.95	19.01
17.5124	0.3346	5.06427	4.01	97.88
18.2692	0.1171	4.85617	22.21	189.51
20.1389	0.1338	4.40934	7.50	73.11
21.1592	0.1673	4.19898	3.46	42.23
23.9718	0.0836	3.71230	5.21	31.75
24.8168	0.2676	3.06176	1.42	27.63
25.6438	0.1338	3.46993	2.09	20.43
27.4289	0.4015	3.24549	0.66	19.42
29.1676	0.2676	3.06176	1.42	27.63
31.0441	0.1338	2.88083	1.77	17.31
35.4420	0.5353	2.53279	1.39	54.33
37.0077	0.3346	2.42916	1.24	30.14
39.5234	0.4015	2.28015	0.72	21.12
57.4083	0.9792	1.60383	0.43	41.38

change of  $\Delta H = 7,450\text{ J g}^{-1}$ , is a combination of two transitions which is in line with TG data. The second transition is an endothermic one starting from  $750\text{ }^{\circ}\text{C}$  and ending at  $950\text{ }^{\circ}\text{C}$  with maximum at  $880.06\text{ }^{\circ}\text{C}$  involves  $\Delta H = 43.37\text{ J g}^{-1}$ .

TG curve of the composite is showing three transitions. The first transition starts from ambient temperatures and ends at  $200\text{ }^{\circ}\text{C}$  with a mass loss of 4.897 % which is as a result of release of moisture. The temperature range of second transition is very small, i.e.,  $200\text{--}250\text{ }^{\circ}\text{C}$  but is very sharp with a mass loss of about 26 %. The mass loss of second transition in case of photoadduct is similar with respect to mass% but the temperature range in case of composite for this decomposition is low. The third transition is a big one starting from  $250\text{ }^{\circ}\text{C}$  and ending at  $750\text{ }^{\circ}\text{C}$ , with a mass loss of 50 %, which may be as a result of loss of inorganic moieties. The residue left behind at  $900\text{ }^{\circ}\text{C}$  is about 17.06 %. The curve runs parallel to  $X$ -axis up to  $1,000\text{ }^{\circ}\text{C}$ , showing the stability of the composite.

The DSC of the composite is showing two transitions, like that of photoadduct, but the nature of these transitions is just reverse of what has been observed in photoadduct. The first DSC transition in case of composite is a small one and endothermic peak from  $100$  to  $300\text{ }^{\circ}\text{C}$  with a maximum at  $227.15\text{ }^{\circ}\text{C}$  giving a  $\Delta H$  value of  $245.5\text{ J g}^{-1}$ , while the other one is an exothermic peak starting from  $300\text{ }^{\circ}\text{C}$  and ending at  $900\text{ }^{\circ}\text{C}$  with a maximum at  $618.11\text{ }^{\circ}\text{C}$  giving  $\Delta H$  value of  $6,186\text{ J g}^{-1}$ . The second exothermic peak is a combination of two peaks, in accordance with the TG data. On comparing the DSC of neat PANI, photoadduct, and composite involving the photoadduct, it is evident that nature of DSC transition in case of composite is different

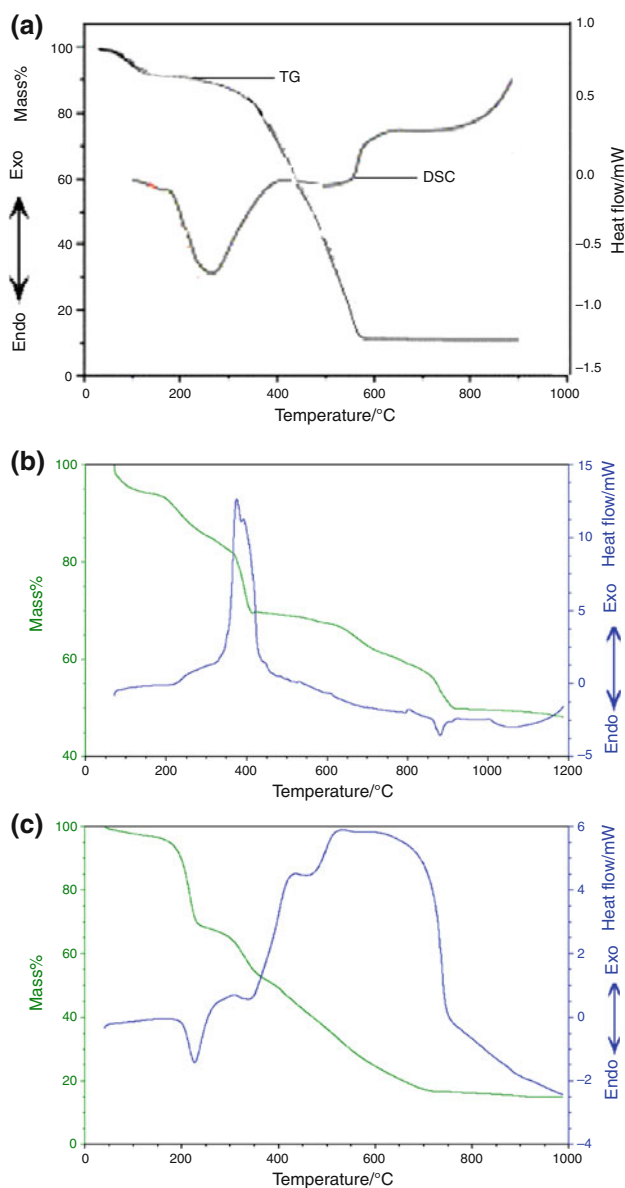


**Fig. 6** TG/DSC of **a** PANI, **b** photoadduct of potassium hexacyanoferrate with hexamine and  $\text{CoCl}_2$ , and **c** composite of potassium hexacyanoferrate with hexamine and  $\text{CoCl}_2$  in PANI

from PANI and photoadduct, thus showing the effect of photoadduct on composite. On comparing the TG curves of PANI, photoadduct, and composite, it is evident that in case of neat PANI complete decomposition of PANI takes place within the temperature range of 550–600 °C. The third transition in case of photoadduct ends at 900 °C and shows stability up to 1,200 °C, while the third transition in case of composite ends at 700 °C, and beyond this temperature, there is no decomposition. TG curve runs parallel to X-axis beyond this point and shows stability up to 1,000 °C, which clearly proves that photoadduct has been inserted into the composite and has increased the thermal stability of the composite material.

## Conclusions

From the study, it is evident that with the procedure mentioned, there is successful synthesis of composite between PANI and photoadduct of potassium hexacyanoferrate involving hexamine and  $\text{CoCl}_2$ . Proper interaction between PANI and photoadduct is proved by FTIR. SEM images are also showing successful synthesis of composite. Thermal stability of composite has increased to a greater extent than that of PANI; hence the material can be used for high-temperature application purposes. Moreover, amorphous structure of PANI has been changed to crystalline structure as shown by XRD, hence proving successful synthesis of composite.

**Acknowledgements** The authors are grateful to Department of Science and Technology, Government of India for financial assistance to carry out this research work under research project No: (SR/NM/NS-97/2008). The authors are also grateful to Prof Rajat Gupta, Director, NIT Srinagar and Prof. Siraj Ahmad, Head Department of Chemistry, NIT Srinagar for help and support.

## References

1. Yuan S, Jaramillo R, Rosenbaum TF, Yu L. Synthesis and characterization of conjugated polymers containing first row transition metal complexes. *Macromolecules*. 2006;39:8652–8.
2. Hongyao X, Shiao WK, Juh SL, Feng CC. Thermal Properties, and  $T_g$  increase mechanism of poly(acetoxystyrene-co-octavinyl-polyhedral oligomeric silsesquioxane) hybrid nanocomposites. *Macromolecules*. 2002;35:8788–93.
3. Liu SJ, Chen Y, Xu WJ, Zhao Q, Huang W. New trends in the optical and electronic applications of polymers containing transition-metal complexes. *Macromol Rapid Commun*. 2012. doi: [10.1002/marc.201100775](https://doi.org/10.1002/marc.201100775).
4. Ley KD, Schanze KS. Photophysics of metal-organic  $\pi$ -conjugated polymers. *Coord Chem Rev*. 1998;171:287–307.
5. Mosner P, Vosejkova K, Koudelka L, Benes L. Thermal studies of  $\text{ZnO-B}_2\text{O}_3\text{-P}_2\text{O}_5\text{-TeO}_2$  glasses. *J Therm Anal Calorim*. 2012; 107:1129–35.
6. Wang SX, Sun LX, Tan ZC, Xu F, Li YS. Synthesis characterization and thermal analysis of polyaniline (PANI)/ $\text{Co}_3\text{O}_4$  composites. *J Therm Anal Calorim*. 2007;89:609–12.
7. Metcalfe C, Thomas JA. Kinetically inert transition metal complexes that reversibly bind to DNA. *Chem Soc Rev*. 2003;32: 215–24.
8. Bharadwaj RK, Berry RJ, Farmer BL. Molecular dynamics simulation study of norbornene-POSS polymers. *Polymer*. 2000;41:7209–21.
9. Xu H, Kuo SW, Lee JL, Chang FC. Glass transition temperatures of poly(hydroxystyrene-co-vinylpyrrolidone-co-isobutylstyryl) polyhedral oligosilsesquioxanes. *Polymer*. 2002;43:5117–24.
10. Phang SW, Tadokoro M, Watanabe J, Kuramoto N. Synthesis, characterization and microwave absorption property of doped polyaniline nanocomposites containing  $\text{TiO}_2$  nanoparticles and carbon nanotubes. *Synth Met*. 2008;158:251–8.
11. Skotheim TA, Dekker M. *Handbook of conducting polymers*. New York: Marcel Dekker; 1986.
12. Datta J, Balas A. DSC and thermal stability investigation of novel poly(ester-ether)glycols and poly(ester-ether)urethanes. *J Therm Anal Calorim*. 2003;74:615–21.

13. Miller LL, Mann KR.  $\pi$ -dimers and  $\pi$ -stacks in solution and in conducting polymers. *Acc Chem Res.* 1996;29:417–23.
14. Hong Y, Mille LL. Electrically conducting polyester that has isolated quatrathiophene units in the main chain. *Chem Mater.* 1995;7:1999–2000.
15. Elisabeth HB, Langveld MW, Ulrich S. New trends in the use of transition metal–ligand complexes for applications in electroluminescent devices. *Adv Mater.* 2005;17:1109–21.
16. Zhang ZM, Wei ZX, Wan MX. Nanostructures of paolyaniline doped with inorganic acids. *Macromolecules.* 2002;35:5937–42.
17. Tsocheva Terlemezyan L. Calorimetric investigations of high density polyethylene/polyaniline composites. *J Therm Anal Calorim.* 2005;81:3–8.
18. Kingsborough RP, Swager TM. Electroactivity enhancement by Redox matching in cobalt salen-based conducting. *Adv Mater.* 1998;10:1100–4.
19. Wang S, Huang Z, Wang J. Thermal stability of several polyaniline/rare earth oxide composites (I): polyaniline/CeO<sub>2</sub> composites. *J Therm Anal Calorim.* 2012;107:1199–203.
20. Nabid MR, Golbabaee M, Bayandori A, Moghaddam R, Dinaryand R. Polyaniline/TiO<sub>2</sub> nanocomposite: enzymatic synthesis and electrochemical properties. *Int J Electrochem Sci.* 2008;3:1117–26.
21. Mohammadi A, Moghaddam AB, Dinarvand R, Badraghi J, Atyabi F, Saboury AK. Electrocatalytic oxidation of sulfite by quinizarine at carbon paste electrode. *Int J Electrochem Sci.* 2008;3:1236–47.
22. Phang SW, Tadokoro M, Watanabe J, Kuramoto N. Microwave absorption behaviors of polyaniline nanocomposites containing TiO<sub>2</sub> nanoparticles. *Curr Appl Phys.* 2008;8:391–4.
23. Muraleedharan K, Kannan MP. Thermal decomposition kinetics of potassium iodate. *J Therm Anal Calorim.* 2011;103:943–55.
24. Ali SI, Majid K. Pyrazine complexes of octacyanometallates of Mo(IV) and W(IV) with 8-hydroxyquinoline: synthesis, characterisation and thermal studies. *J Therm Anal Calorim.* 1999;58:153–65.
25. Wang N, Zhang XR, Zhu DS, Gao JW. The investigation of thermal conductivity and energy storage properties of graphite/paraffin composites. *J Therm Anal Calorim.* 2012;107:949–54.
26. Ali SI, Majid K. Characterization, kinetics and mechanism of thermal decomposition of photosubstituted ethylenediamine complexes of molybdate(IV) and tungstate(IV) with chromium(III). *Thermochim Acta.* 1998;317:183–92.
27. Vogler A, Kunkely H. Electronic spectra and photoreactivity of cyclopentadienyl complexes. *Coord Chem Rev.* 2001;211:223–33.
28. Kong J, Franklin NR, Zhou C, Chapline MG, Peng S, Cho K, Dai H. Nanotube molecular wires as chemical sensors. *Science.* 2000; 87:622–5.
29. Szlarzewicz J, Samotus A. Photochemical reactions of molybdenum m and tungsten octacyanometallates(IV) in acidic aqueous media containing 2,2'-bipyridyl or 1,10-phenanthroline. *Transition Met Chem.* 1995;20:174–8.
30. Majid K, Rafiqi FA, Rather MS. Photo substituted synthesis, characterization and thermal kinetics of potassium hexacyanoferrate with monoethanolamine. *Elixir Chem Phys.* 2011;36: 3245–7.
31. Majid K, Awasthi S, Singla ML. Low temperature sensing capability of polyaniline and Mn<sub>3</sub>O<sub>4</sub> composite as NTC material. *Sens Actuators, A.* 2007;135:113–8.